# Perfect State Transfer in Spin Chains with On-Site Energy Parametrization

**Abdulfateh Bezaz**

*Master by Research*
*University Of York*
*Physics, Engineering and Technology*
*November 2022*

**Abstract**

In the past decade, theoretical work on spin chains has made substantial progress in the search for systems that can attain high-fidelity quantum information transfer. We extend previous work on tuning the coupling between sites in spin chains by investigating how high-fidelity information transfer may occur by modifying the on-site energies. We show that, given the right spectrum, perfect state transfer may be achieved by modifying only the diagonal elements of the XY Hamiltonian. Furthermore, a genetic algorithm was also utilized in this study, which demonstrated that merging A.I and physics may provide fantastic findings and, in the future, can help us investigate far larger scientific challenges. The incentives for investigating on-site energies are significant because achieving and maintaining perfect state transfer by tuning solely the couplings for some physical systems might be difficult. The study detailed in this thesis aims to bring us one step closer to understanding the many applications of spin chains in quantum information systems.

# Contents

# List of Figures

# List of Tables

# Acknowledgements

I'd like to express my sincere appreciation to my supervisors, Irene D'Amico, Timothy Spiller, and Marta Estarellas, for their patience and consistent guidance during this project. Professor Timothy Spiller provided concise analytical notes and explanations for me to understand as well as research guidance, Professor Irene D'Amico provided much guidance and expertise in directing my research goals and tasks, and Dr Marta Estarellas provided guidance in my research tasks along with helping me use the genetic algorithm she co-developed.

# Declaration of Authorship

I declare that this thesis is an original work of which I am the only author. This work has never been nominated for an award at this or any other university. All sources used in this thesis are cited as references.

# 1 Introduction

Quantum mechanics is becoming more significant in the formation of new and more efficient computer technologies; it underpins the operation of classical computers and communication devices, from the transistor to the most recent hardware improvements that increase the speed and power of computer and communications components. Until recently, quantum mechanics' influence was limited to low-level implementation; it had little impact on how computing or communication was thought of or investigated. The notion that quantum computing may outperform conventional computing arose in the late twentieth century when certain bottlenecks in classical computing emerged. It was later suggested by Feynman and other physicists that perhaps quantum phenomena may be better simulated on quantum computer designs [1]. Aside from modelling quantum physics, newly discovered quantum algorithms were being used to address problems that can be solved in polynomial time where quantum algorithms could solve these challenges much better than classical techniques [2, 3]. Peter Shor, a pioneer in quantum computing, revealed that his quantum algorithm beats any classical technique in determining prime factors of very large numbers [4]. Shor's conclusion attracted a lot of attention to the subject, and questions about its practical importance remained since quantum systems are notoriously sensitive. Processing and manipulating quantum information for computing is a daunting task due to decoherence and the inherent sensitivity of quantum systems, where many quantum information processing methods rely on quantum state transfer between sites in coherent time. Photon transmission is the most frequent method of transferring quantum information, and it is widely used in quantum entanglement methods for communication and cryptography applications, such as quantum key distribution [5, 6]. However, the deployment of solely photonic systems for the processing, manipulation, and transfer of quantum information across short distances may be difficult since photons do not constitute a network of interacting states; rather, they operate as carriers [7]. Quantum information in a computer must be processed between registers separated by exceptionally small distances on a network. As a result, we should investigate other techniques of processing quantum information. Spin chain models are one solution given to this problem [8, 9, 10, 11, 12, 13, 14, 15, 16, 17, 18]. In a spin chain, quantum information is transferred via natural dynamics. In physical systems, this may be accomplished by any permanently coupled two-level states chained together by some exchange interaction, such as ion traps [19], chains of superconducting qubits [20, 21, 22] or a sequence of external RF pulses which was proposed in [23] to drive single-spin quantum information down a chain of Ising-coupled spins. In this study, we extend prior work on tuning the coupling between sites in spin chains by studying how high-fidelity information transmission may occur by adjusting the on-site energies instead. The rationale for investigating on-site energies is important because achieving high-fidelity quantum state transfer by tuning just the couplings for certain physical systems may be difficult to achieve and maintain. Consider the technical challenges of managing neighbour interac-

tions with complex molecules. For some systems, such as ion traps, keeping the couplings constant while changing the on-site energies may be simpler. This study investigates the ability to generate perfect state transfer purely by adjusting the configuration of on-site energies, with the interaction between sites remaining constant and unchanged.

## 1.1 Classical vs Quantum Computing

With the invention of digital information and transistors in the past century, civilisation underwent a technological revolution. Computers are now so deeply embedded in modern civilization that without them, the mechanisms that regulate most aspects of human lives would collapse. However, traditional computers have intrinsic constraints, such as their ability to do certain large computations quickly, memory storage, encryption techniques, and the inevitable end of Moore's law [24]. As chip sizes approach 10 nm, the quantum nature of electrons must be considered, and classical physics can no longer adequately maintain these systems due to the emergence of quantum fluctuations and errors. Quantum computers operate in a profoundly different fashion than classical computer architectures [25]. Instead of bits, which can only represent binary data, quantum computers use qubits, which are a superposition of $|0\rangle$ and $|1\rangle$. The advantage of a quantum computer is due to the exponential growth in processing power as a function of the number of qubits, whereas the power of a classical computer is highly dependent on the transistor count. They are also superior at protecting private information through quantum encryption protocols [26]. As civilization becomes more complex, technology must be capable of keeping pace. Quantum computers have the potential to once again transform how humans live; we might have significantly more powerful artificial intelligence than present models, as well as better tools for modelling physical processes, which may lead to an increase in scientific discoveries. However, quantum computers are currently incredibly difficult to maintain and develop [27]. This is owing to a variety of issues, including existing constraints on superconducting materials, which must be held at extremely low temperatures. Decoherence and the general sensitivity of quantum systems are also significant drawbacks since physicists must devise novel methods to rectify and compensate for information loss due to decoherence [28, 29, 30].

## 1.2 The Qubit

Quantum bits, like bits in classical information, are fundamental units of information in quantum information processing. A qubit can be expressed as a superposition of two states and their associated probabilities $\mid \alpha \mid^2 + \mid \beta \mid^2 = 1$ that exist in $\mathbb{C}^2$

$$|\psi\rangle = \alpha\,|0\rangle + \beta\,|1\rangle\,, \tag{1}$$

where $|0\rangle = \left(\begin{smallmatrix}1\\0\end{smallmatrix}\right)$ and $|1\rangle = \left(\begin{smallmatrix}0\\1\end{smallmatrix}\right)$. Physical implementations include the spin-up and spin-down states of the electron, or any two-level quantum system that can be represented as

equation (1). In practice, one must consider multi-party quantum systems such that the Hilbert space for $n$ qubits is then spanned by $2^n$ states such that

$$\mathcal{H} = \mathbb{C}^2 \otimes \mathbb{C}^2 ... \otimes \mathbb{C}^2 = \mathbb{C}^{2^n}, \tag{2}$$

for instance, a system of $n = 2$ qubits must be described using four basis vectors,

$$\begin{aligned} &|0\rangle \otimes |0\rangle \\ &|0\rangle \otimes |1\rangle \\ &|1\rangle \otimes |0\rangle \\ &|1\rangle \otimes |1\rangle \end{aligned} \tag{3}$$

where,

$$\mathcal{H} = \mathbb{C}^2 \otimes \mathbb{C}^2. \tag{4}$$

A quantum $n$-qubit system can be in any arbitrary superposition of the $2^n$ states $|000...0\rangle$ through $|111...1\rangle$. To simplify notation $|i\rangle \otimes |j\rangle$ will be written as $|ij\rangle$.

## 1.3 Pure States and Mixed States

A quantum state's purity can be characterised with the following inequality

$$1/d \leq \xi \leq 1 \tag{5}$$

where $\xi = tr(\rho^2)$, and considered a pure state when equal to unity, i.e. $\rho^2 = \rho$, and $d$ is the dimensions of the state space. A pure state can be represented by the density matrix

$$\rho = |\psi\rangle \langle\psi| , \tag{6}$$

and a mixed state by the matrix

$$\rho_m = \sum p_i |\psi_i\rangle \langle\psi_i| , \tag{7}$$

where the coefficient $p_i$ is the probability amplitude of finding a pure state in the overall mixed state and satisfies the general normalization rule. The inequality (5) has an upper bound of $tr(\rho) = 1$ representing a pure state, and the lower bound reflecting a totally mixed state as the matrix $\rho_{tm} = \frac{1}{d} I_d$.

## 1.4 Quantum Gates

A quantum gate can be defined as unitary operations on a qubit state that are analogous to classical logic gates; every quantum algorithm, under the gate-based model of quantum computation, may be described as a sequence of these actions. In mathematical terms, these are simply matrices acting on a vector. For example, the Pauli matrix $X = \left(\begin{smallmatrix} 0 & 1 \\ 1 & 0 \end{smallmatrix}\right)$ is analogous to the classical logic gate NOT.

## 1.5 Perfect State Transfer

Perfect State Transfer is the terminology used when a quantum information system is able to transfer a quantum state from A to B with fidelity of unity. Fidelity is a metric for measuring the *proximity* between states and is critical for understanding how successfully quantum information is transmitted. The fidelity of a generalized mixed system given by density operators $\rho$ and $\rho'$ is of the form

$$F(\rho, \rho') = \left( tr\sqrt{\sqrt{\rho}\rho'\sqrt{\rho}} \right)^2 . \tag{8}$$

It becomes more clear to see how fidelity measures the proximity if $\rho$ and $\rho'$ are converted to pure states $\rho = |\psi_i\rangle \langle\psi_i|$ and $\rho' = |\psi_j\rangle \langle\psi_j|$ such that

$$F(\rho, \rho') =| \langle\psi_i|\psi_j\rangle |^2, \tag{9}$$

then if $\rho = \rho'$,

$$F(\rho, \rho') =| \langle\psi_i|\psi_i\rangle |^2 = 1. \tag{10}$$

Because the states in spin chains are time-dependent. The fidelity in this situation is the inner product of the actual initial state and the predicted transferred state under some time evolution. Imagine a spin chain constructed with all states in their ground state, $|0\rangle$. At t=0, an initial excitation $|\psi\rangle_A = |1\rangle_A$ is injected at some site A ($|0\rangle \longrightarrow |1\rangle$), which will travel through the natural dynamics of the spin chain until the final state $|\psi\rangle_B = |1\rangle_B$ at site B is observed. For such a system, the fidelity may be expressed as follows:

$$F(t) =| \langle\psi_B| e^{-i\mathcal{H}t/\hbar} |\psi_A(0)\rangle |^2 . \tag{11}$$

It should now be clear that the fidelity between states must equal unity for spin chains to be maximally effective in computer topologies. This would imply that the quantum state was transmitted without error or information loss from point A to point B. This is clearly impossible due to the overall sensitivity of quantum systems; nevertheless, thanks to the use of quantum error correcting codes, we can still compensate for some loss of information.

## 1.6 Spin Chain Models

Spin chains, in general, are chains of coupled two-level quantum systems that have an exchange interaction or spin interaction between neighbours. For a visual reference, figure 1 illustrates a one-dimensional spin chain with nearest-neighbour coupling. Spin chain models are particularly precise in modelling 1-dimensional nearest-neighbour interactions. Magnetic phenomena such as ferromagnetism and anti-ferromagnetism, for example, can

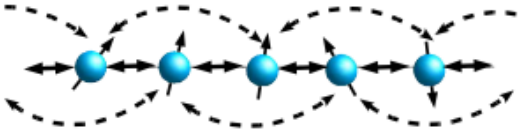

Figure 1: A system of spins that are permanently coupled to one other through some exchange interaction.

be accurately explained using spin chain models since the spin interaction between neighbours is what results in alignment or anti-alignment between site moments. The XYZ Hamiltonian, which is the generic Hamiltonian for such systems, may be expressed as

$$\mathcal{H}_{XYZ} = -\frac{1}{2}\sum_{i=1}^{N}\sum_{\mu} J_{i,i+1}^{\mu}\sigma_i^{\mu}\sigma_{i+1}^{\mu}, \tag{12}$$

where $\mu = x, y, z$, $\sigma_i^{\mu}$ are the Pauli matrices, and $J_{i,i+1}$ is the coupling strength between sites i and i+1. If we now consider the coupling strength $J_{i,i+1}^{\mu}$ in $\mu = x, y, z$, we can start to imagine how different types of models may arise. The main difference between models is determined by $J_{i,i+1}^{\mu}$. If $J^x = J^y = J^z$, the model is termed the isotropic XYZ Hamiltonian; if $J^x = J^y \neq J^z$, it is called the anisotropic XXZ Hamiltonian; if $J^z = 0$ and/or $J^x = J^y$, it is coined the XY or XX Hamiltonian; and lastly, when $J^x = J^y = 0$, it is called the Ising Hamiltonian. These many theoretical models have been extensively researched in the past to describe a wide range of phenomena related to coupled spins; however, for the sake of this study, we will concentrate on the XY spin chain model, which we can now represent in a different form

$$\mathcal{H}_{XY} = \frac{1}{2}\sum_{i=0}^{N-1} J_i(\sigma_i^x \cdot \sigma_{i+1}^x + \sigma_i^y \cdot \sigma_{i+1}^y) + \frac{1}{2}\sum_{i=0}^{N} h_i(\sigma_i^z + I), \tag{13}$$

where $\sigma^x, \sigma^y$ and $\sigma^z$ are the respective Pauli matrices, $J_i$ the coupling strength between sites, and for completeness, the term $\sum_{i=0}^{N} h_i(\sigma_i^z + I)$ has been added which is a representation of an external magnetic field acting on the chain, with $h_i$ being the external field energy of some qubit at some site i. More broadly, for one-dimensional models, the Jordan-Wigner transformation, which emerges from transforming Pauli matrices to creation and annihilation operators, is one technique for formulating this Hamiltonian in a variety of distinct but equivalent ways such as

$$\mathcal{H}_{XY} = \sum_{i=0}^{N-1} J_i(a_i^{\dagger}a_{i+1} + a_{i+1}^{\dagger}a_i) + \sum_{i=0}^{N} h_i a_i^{\dagger}a_i. \tag{14}$$

We can further transform this Hamiltonian into a form more convenient for our uses by setting $\sigma^x = |1\rangle\langle 0| + |0\rangle\langle 1|$, $\sigma^y = i(|1\rangle\langle 0| - |0\rangle\langle 1|)$ and $\sigma^z = |1\rangle\langle 1| - |0\rangle\langle 0|$, setting $h_i \longrightarrow \epsilon_i$ and finally, using the encoding

- Spin-up, $|\uparrow\rangle = |1\rangle$
- Spin-down $|\downarrow\rangle = |0\rangle$

$\mathcal{H}_{XY}$ can be written as,

$$\mathcal{H}_{XY} = \sum_{i=1}^{N-1} J_{i,i+1}[|1\rangle\langle 0|_i \otimes |0\rangle\langle 1|_{i+1} + |0\rangle\langle 1|_i \otimes |1\rangle\langle 0|_{i+1}] + \sum_{i=1}^{N} \epsilon_i |1\rangle\langle 1|_i , \tag{15}$$

where $\epsilon_i$ is the energy required to excite $|\downarrow\rangle_i$ to $|\uparrow\rangle_i$, and $J_{i,i+1} > 0$ is the exchange interaction between sites $i$ and $i+1$. If we try to physically analyze (15), we may deduce that the first Hamiltonian term is the hopping between sites, while the last term represents the on-site energy corresponding to a spin in state $|1\rangle$. This will be the preferred form of $\mathcal{H}_{XY}$ used throughout this study.

## 1.7 The Standard Criteria for a Quantum Computer

The current benchmark for what constitutes a successful quantum computer is a set of criteria devised by theorist David P. DiVincenzo [31]. Seven physical conditions must be satisfied in this criterion, which is outlined as follows:

- A scalable physical system with well-characterized qubits.
- The ability to initialize the state of the qubits to a simple fiducial state.
- Long relevant decoherence times.
- A universal set of quantum gates.
- A qubit-specific measurement capability.
- The ability to interconvert stationary and flying qubits.
- The ability to faithfully transmit flying qubits between specified locations.

### 1.7.1 A Physically Scalable System with Well-Characterized Qubits

A well-characterized system necessitates a thorough knowledge of the system, implying that the system can be modelled and recreated physically. The spin chains under consideration in this work, for example, are well described since we can generate comprehensive analytical solutions to their Hamiltonians. Second, we require scalability, which includes the capacity to handle and manipulate huge $n$-qubit systems. Physicists are now highly competent at building well-characterized systems; but, scalability is a challenge. Because

we have barely scratched the surface with low-qubit devices, it is still uncertain if our existing quantum technology is scalable.

### 1.7.2 Initializing the Qubit States

This criterion is critical because we need to process and measure qubits between locations. As a result, we must be able to initialize the qubits in a well-defined state, which is the spin-down state, $|0\rangle$ in our instance. In many circumstances, initialization is carried out by preparing the system in its ground state. When it comes to quantum error correction methods, ground states are especially important since they demand a huge supply of freshly initialized qubits.

### 1.7.3 Long Relevant Decoherence Times

One of the main challenges in quantum computing is the information loss of a quantum system to the environment, otherwise known as decoherence. The coherence time is the typical time it takes for a state to keep its information. It is critical that the coherence time is substantially longer than the time required to perform a qubit operation. If this is not the case, all quantum information will be lost to the environment before the procedure is completed.

### 1.7.4 A Universal Set of Quantum Gates

Single-qubit gates are manipulations on a single qubit, whereas two-qubit gates entangle two qubits. The capacity to perform both of the aforementioned gates on all of the system's qubits is thus defined as a universal gate set.

### 1.7.5 A Qubit-Specific Measurement Capability

Quantum computers require the capacity to calculate quantum algorithms and permit the transfer of qubits; as a result, the outcome of a consequent calculation must be measured. The Elzerman technique, which performs a one-shot electrical measurement of the state of a single electron spin in a semiconductor quantum dot, may be used to measure spin qubits [32].

# 2 Methods

The numerical findings in this work were achieved by a genetic algorithm that optimizes the spin chain's Hamiltonian parameters [33]. The genetic algorithm's objective in this use case is to optimize the neighbour interaction between sites as well as on-site energies in order to arrive at a solution with perfect state transfer between two specified sites. Furthermore, the spin chain dynamics are calculated via direct diagonalization of $\mathcal{H}_{XY}$ with symmetry imposed, enabling us to compute time-dependent solutions. The genetic algorithm will optimize a solution to the best of its ability to produce perfect state transfer, modulating certain parameters such as the coupling between sites, and the on-site energies. What's significant to explore here is how on-site energy configurations might build systems that produce high-fidelity information transmission, providing engineers with another tool to employ in the physical implementation of these systems.

## 2.1 Dynamics of a Spin Chain

As the reader is probably aware, the initial step in most quantum mechanics research problems is effectively solving the Schrödinger equation such as

$$i\hbar\frac{\partial}{\partial t}\left|\psi(t)\right\rangle = \mathcal{H}(t)\left|\psi(t)\right\rangle. \tag{16}$$

The spin chain systems in this study will be considered ideal quantum systems, i.e., uncoupled from the environment. That is, it is entirely closed, and so the Hamiltonian remains independent of time. Practically, however, solutions have been proposed to counter the loss of information. Advancements have demonstrated the successful utilization of quantum error correction techniques for transmitting a qubit with high fidelity over an imperfect chain. This method involves employing multiple imperfect spin chains in parallel, enabling the transmission of qubits over distances significantly larger than the localization length of individual chains [34]. In a comprehensive review by Stolze [35], the focus is placed on the analysis of manufacturing errors affecting the nearest-neighbour spin couplings. The review explores potential strategies for overcoming these errors by utilizing boundary-controlled chains and other methods. This insightful examination sheds light on the methods that can be employed to address and mitigate the impact of manufacturing errors on the performance of spin systems.

To begin solving equation (16), consider the time-independent Schrödinger equation for a basis state $\left|\phi_n\right\rangle$

$$\mathcal{H}\left|\phi_n\right\rangle = E_n\left|\phi_n\right\rangle. \tag{17}$$

Using the fact that the set of $\phi_n$ is complete, the time-dependent solution can be written in terms of the basis vectors such that,

$$\left|\psi(t)\right\rangle = \sum_n \zeta_n(t)\left|\phi_n\right\rangle, \tag{18}$$

where the coefficients $\zeta_n(t) = \langle\phi_n|\psi(t)\rangle$ contain the dependence on time. We can transform the Schödinger equation by now considering the basis states $|\phi_n\rangle$ such that,

$$i\hbar\frac{\partial}{\partial t}\langle\phi_n|\psi(t)\rangle = \langle\phi_n|\,\mathcal{H}\,|\psi(t)\rangle\,, \tag{19}$$

and now in terms of the coefficient $\zeta_n(t)$ as follows

$$i\frac{\partial}{\partial t}\zeta_n(t) = E_n\zeta_n(t)\ . \tag{20}$$

This equation may then be solved as a time-dependent first-order differential equation, yielding a solution for $\zeta_n(t)$ which we can now use to find a wavefunction solution that is time-dependent in terms of these coefficients

$$|\psi(t)\rangle = \sum_n \zeta_n(0)e^{-iE_nt}\,|\phi_n\rangle\,. \tag{21}$$

By remembering that $|\psi(t)\rangle = \sum_n \zeta_n(t)\,|\phi_n\rangle$, the time-dependent solution $|\psi(t)\rangle$, can be found by diagonalizing the Hamiltonian to find the eigenstates in order to find the solution in terms of $\zeta_n(0)$, which is $\zeta_n(0) = \langle\phi_n|\psi(0)\rangle$.

## 2.2 Perfect State Transfer in Systems with Mirror Symmetry

Perfect state transfer requires fidelity of unity between the initial state and the desired "destination" state. This is typically accomplished by imposing mirror symmetry in the states $[\mathcal{H}, \mathcal{M}] = 0$, where $\mathcal{M}$ is defined as the operator that mirrors the chain's state about its centre point. To highlight further the implications of mirror symmetry consider the following analytical description for a system with basis states $|v_j\rangle$

$$\mathcal{H}\,|v_j\rangle = E_j\,|v_j\rangle\,, \tag{22}$$

and

$$\mathcal{M}\,|v_j\rangle = \pm\,|v_j\rangle\,. \tag{23}$$

Since $[\mathcal{H}, \mathcal{M}] = 0$, the states $|v_j\rangle$ are eigenstates of both $\mathcal{H}$ and $\mathcal{M}$. We can define a state that is a superposition of a normal state and mirrored state as such,

$$|\psi_\pm\rangle = |\psi\rangle + \mathcal{M}\,|\psi\rangle\,, \tag{24}$$

and,

$$\mathcal{M}\,|\psi_\pm\rangle = \mathcal{M}\,|\psi\rangle \pm \mathcal{M}^2\,|\psi\rangle\,. \tag{25}$$

Since $\mathcal{M}^2 = \mathbb{I}$ We obtain,

$$\mathcal{M}\,|\psi_\pm\rangle = \pm\,|\psi_\pm\rangle\,, \tag{26}$$

we are then left with even and odd parts for any state $|\psi\rangle$

$$|\psi\rangle = \frac{1}{2}, (|\psi_+\rangle + |\psi_-\rangle), \tag{27}$$

and

$$\mathcal{M}\left|\psi\right\rangle = \frac{1}{2}(\left|\psi_{+}\right\rangle - \left|\psi_{-}\right\rangle). \tag{28}$$

Therefore if the spectrum allows, we can achieve complete mirroring of the initial state and thus generate perfect state transfer. Through the diagonalization of $\mathcal{H}_{XY}$ we can obtain even and odd time-dependent solutions in terms of the eigenstates $\left|v_j\right\rangle$ such that,

$$\left|\psi\right\rangle_{+} = \sum_{j+} a_{j+} e^{-i\omega_j t}\left|v_{j+}\right\rangle, \tag{29}$$

and

$$\left|\psi\right\rangle_{-} = \sum_{j-} a_{j-} e^{-i\omega_j t}\left|v_{j-}\right\rangle, \tag{30}$$

where $\omega_j = E_j$ in natural units, $\hbar = 1$, and the subscript $+$ refers to an even state and - to an odd state. This description shows the mirroring between states which entails periodicity in the dynamics. The odd and even states evolve as $\left|\psi\right\rangle_{+} \longrightarrow e^{i\alpha}\left|\psi\right\rangle_{+}$, and $\left|\psi\right\rangle_{-} \longrightarrow e^{i(\alpha+\pi)}\left|\psi\right\rangle_{-}$ for some global phase $\alpha$. Therefore, the state $\left|\psi\right\rangle \longrightarrow e^{i\alpha}(\left|\psi\right\rangle_{+} - \left|\psi\right\rangle_{-}) = e^{i\alpha}\mathcal{M}\left|\psi\right\rangle$ will have unit fidelity against its mirrored version $\mathcal{M}\left|\psi\right\rangle$ since the phase factor $e^{i\alpha}$ will be eliminated upon calculating the inner product between the two states.

## 2.3 Spectrum of $\mathcal{H}_{XY}$ for PST using a Coupling Profile

In the research area of spin chains, it is known that fixed configurations of the spin coupling following the profile $J_{i,i+1} = J_0\sqrt{i(N-i)}$ can generate perfect state transfer over arbitrary distances [36, 37]. In the XY spin chain, mirror symmetry implies a focal symmetry between sites A and B. It's worth noting how this symmetry affects the spectrum of energy eigenvalues. It can be demonstrated that for such systems to provide perfect state transfer, the ratios of the differences of the eigenvalues must be rational [37]. Consider an initial state $\left|\zeta\right\rangle$ after some time $\tau_0$; in natural units, the state may be written as

$$e^{-iH\tau_0}\left|\zeta\right\rangle = e^{i\phi}\left|\eta\right\rangle. \tag{31}$$

If $[\mathcal{H}, \mathcal{M}] = 0$, where $\mathcal{M}$ is the mirror operator, then if (31) evolves once more under some mirroring time $\tau_0$,

$$e^{-iH2\tau_0}\left|\zeta\right\rangle = e^{-iH\tau_0}e^{i\phi}\left|\eta\right\rangle = e^{i2\phi}\left|\zeta\right\rangle. \tag{32}$$

The periodicity shown in the arguments of equation (32) is a fundamental condition for $F(t) = 1$ systems with imposed $[\mathcal{H}, \mathcal{M}] = 0$. If a state $\left|\psi\right\rangle$ with this periodicity is considered, the following equation is obtained,

$$\left|\psi(2\tau_0)\right\rangle = \sum_j a_j e^{-i2E_j\tau_0}\left|j\right\rangle = e^{i2\phi}\sum_j a_j\left|j\right\rangle, \tag{33}$$

where $E_j$ are the energy eigenvalues of $\mathcal{H}_{XY}$. For all stationary states, there exists the following periodicity condition that needs to be fulfilled

$$2E_i\tau_0 - 2\phi = 2n_i\pi. \tag{34}$$

We can then take $\phi$ out of the equation to produce the following expression,

$$(E_i - E_j)2\tau_0 = 2\pi(n_i - n_j), \tag{35}$$

and if $\tau_0$ is eliminated from equation (35) we obtain an expression for the spectrum

$$\frac{E_i - E_j}{E_{i'} - E_{j'}} = \frac{n_i - n_j}{n_{i'} - n_{j'}} \in \mathbb{Q}. \tag{36}$$

Since $n_i \in \mathbb{Z}$, this implies a symmetric system capable of perfect state transfer must be periodic and that the ratios of the separation of eigenvalues be rational. In the case of the Christandl *et al* coupling profile $J_{i,i+1} = J_0\sqrt{i(N-i)}$ [36, 37], the eigenvalues are equally separated. As an analytical example of how such a spectrum can generate PST, consider a spin chain of N=4 sites, with the following spectrum,

$$E_j = 3\Delta, \Delta, -\Delta, -3\Delta. \tag{37}$$

Each eigenvalue is of equal separation $2\Delta$, where $\Delta$ is some constant. Now consider the consequence of this spectrum on the wavefunctions,

$$|\psi(t)\rangle_+ = a_{3\Delta}e^{-i3\Delta t}\,|u_{3\Delta}\rangle + a_{-\Delta}e^{i\Delta t}\,|u_{-\Delta}\rangle\,, \tag{38}$$

and

$$|\psi(t)\rangle_- = a_{\Delta}e^{-i\Delta t}\,|u_{\Delta}\rangle + a_{-3\Delta}e^{3i\Delta t}\,|u_{-3\Delta}\rangle\,. \tag{39}$$

If $t = \pi/2\Delta$ we have the following dynamics for odd and even states,

$$|\psi(\pi/2\Delta)\rangle_+ = e^{i\pi/2}\Big(a_{3\Delta}\,|u_{3\Delta}\rangle + a_{-\Delta}\,|u_{-\Delta}\rangle\Big), \tag{40}$$

and

$$|\psi(\pi/2\Delta)\rangle_- = -e^{i\pi/2}\Big(a_{\Delta}\,|u_{\Delta}\rangle + a_{-3\Delta}\,|u_{-3\Delta}\rangle\Big). \tag{41}$$

The odd states must all obtain a negative sign relative to the even states in order for the overall state to mirror the centre of the chain. The symmetry of the eigenstates must invert as a qubit travels over the spectrum, with the same phases, to ensure fidelity of unity between the states at time $\pi/2\Delta$.

## 2.4 The Genetic Algorithm

A genetic algorithm evolves a population of candidate solutions to superior solutions to an optimization problem and belongs to a family of evolutionary algorithms [38, 39, 40, 41, 42, 43, 44, 45]. Each prospective solution contains a set of attributes (its genome) that may be mutated and altered according to natural selection. The evolution process typically begins with a population of randomly created individuals and is iterative, with the population in each iteration referred to as a generation. Every genome in the population's fitness is evaluated in each generation. The fittest individuals are chosen at random from the existing population, and their genomes are tweaked to generate a new generation. The fresh generation of potential solutions is then employed in the algorithm's following iteration. Typically, the method algorithm will stop once good fitness is reached. They are a subset of evolutionary algorithms and are frequently used to produce very good solutions to optimization challenges. For example, in order to find the most optimized positions of the magnetic axis and the X point in an axisymmetric equilibrium, a genetic algorithm was applied to the modellings of magnetically confined toroidal plasmas [46]. Genetic algorithms replicate natural selection, implying that genomes that can adapt to changes in their environment survive, reproduce, and carry on to the next generation. In other words, in order to solve a problem, they duplicate "survival of the fittest" among individuals of consecutive generations. In the search space, an individual is analogous to a chromosome in biology, with each unique gene stored in a string of numbers and letters, as seen in figure 2. These algorithms are generally more robust than traditional A.I methods [47]. Genetic algorithms have also been shown to be useful in researching quantum theory. Heras *et al.* demonstrated that genetic algorithms may be used to improve the fidelity and optimize the resource needs of digital quantum simulation protocols while responding to experimental restrictions. Furthermore, they also show that the GA eliminates not only digital but also experimental mistakes in quantum gates [48]. In the optimization process, five parameters are used as follows,

- Population initialization, the first phase in the Genetic Algorithm Process. The first generation is normally generated at random.
- The fitness function determines how near a particular solution is to the ideal solution. This function is generally customized to a specific problem and allows the algorithm to evaluate fitness scores that determine the survival of a genome.
- Crossover, an operator called crossover is used to change the programming of a chromosome or chromosomes from one generation to the next. Sexual reproduction is achieved by crossover. To create superior progeny, two strings are chosen at random from the mating pool to crossover.
- Selection, the step of a genetic algorithm in which individual genomes from a population are selected for subsequent breeding by the cross-over operator.

- Mutation, an operator used to preserve genetic variation in a population of genomes from one generation to the next.

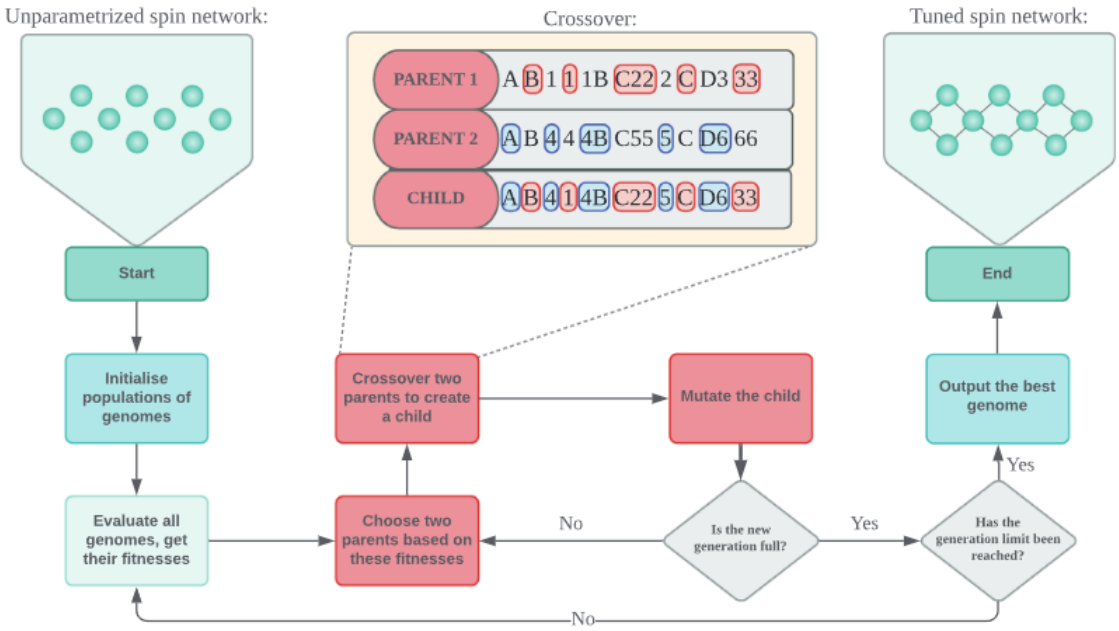


Figure 2: A schematic of the strategy utilized to crossover two genomes. For each character in the child genome, the equivalent character from one of the parents is utilized, with equal probability.

### 2.4.1 Encoding the Genomes into Spin Chains

The spin chain genomes chosen to depict are fixed-sized linear strings of letters and numbers, divided into portions containing relevant information for the optimization process [33]. Sites and their related basis vectors are represented by letters, whereas coupling energies and on-site energies are represented by numbers as shown in figure 3. In the first example, we have states $\langle A|C\rangle$ in the configuration of $\langle A|C\rangle$AB500BC500. This can be translated as the network of a two-level quantum system where the initial state is $|\Psi(0)\rangle = |1\rangle_A$ and the final state for the information to transfer to is $|\Psi_{target}\rangle = |1\rangle_C$ coupled as shown. We can represent on-site energies simply by repeating a letter and using a number to denote the on-site energy, as an example, $\langle A|C\rangle$AB500BC500AA500BB500CC500 represents the same chain as figure 3 but now with on-site energies at each site.

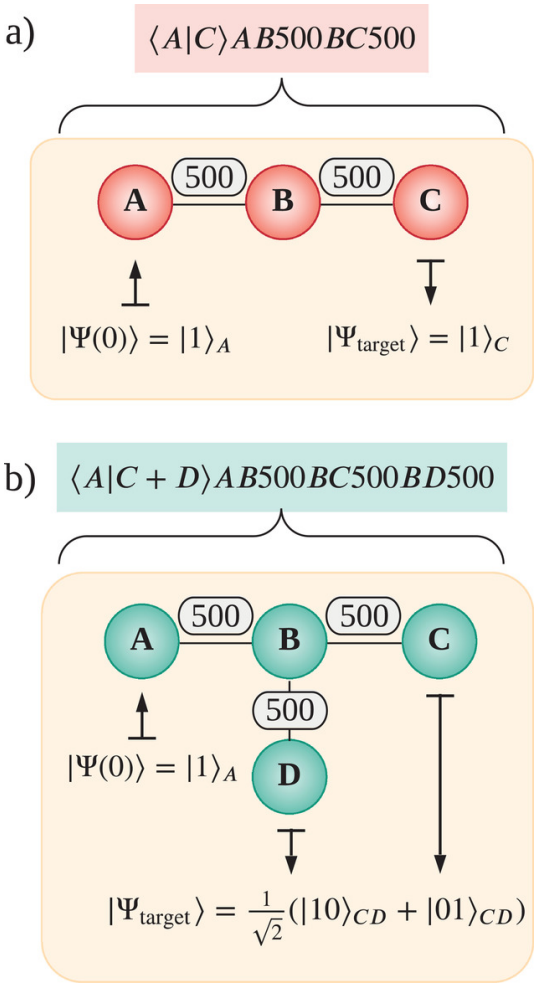


Figure 3: An illustration of the spin chains encoded as genomes, where the couplings are represented by the numbers in between letters which are single excitation basis vectors of the spin chain.

### 2.4.2 Optimizing the Spin Chains

The genetic algorithm has the ability to optimize both the diagonal and non-diagonal elements of $\mathcal{H}_{XY}$ while also offering other constraints via parameters that are customizable [33]. As discussed previously, the genetic algorithm will find high-quality genomes via the fitness function,

$$f(F_{max}, t_f) = 100e^{a(F_{max}-1)}e^{bt_f J_{max}}. \tag{42}$$

The function is exponential so a minor fidelity increase will exaggerate the fitness score. It is also important to note that the function favours short transfer times since in quantum devices one of the main objectives is avoiding decoherence by transferring information before the time it takes for decoherence to occur. $F_{max}$ is the maximum fidelity, $t_f$ in units of $J_{max}^{-1}$ is the time it takes to reach $F_{max}$, and $a, b$ are parameters that modify the output based on what is prioritized, i.e time or fidelity, a suitable $a$ may be chosen

such that the function favours precision since the dependency on $F_{max}$ in the argument of the fitness function weakens once $(1 - F_{max}) < 1/a$, therefore, $a$ was chosen to equal ten such that efficiency and high fidelities with the respect to the information transfer between states is achieved. The parameter $b$ is chosen to reduce the time of information transfer between states. $b$ is a parameter that has more of a strong effect on the transfer time, a larger $\mid b \mid$ will emphasize a smaller transfer time but a sacrifice in the fidelity is unavoidable. In the calculations, a range of $b$ was chosen, from -0.001 to -0.000001 for larger N chains. The algorithm thus uses the fitness function to decide whether a spin chain will be allowed to evolve and contribute to the final solution. This results in a final spin chain with fully optimized $J_{i,i+1}$ and $\epsilon_i$.

### 2.4.3 The Crossover Operation and Reproduction of Genomes

Crossover occurs when two genomes are chosen and merged. It is worth noting that only the numerical values differ that being either the coupling or in this case mainly the on-site energies. Iteratively, this crossover/mutation of the child genome happens by raising or lowering one of its numerical values by a random integer less than or equal to $\mu$, the maximal mutation size. The goal of the iterations is to go from $\mu_i$ to $\mu_f$. So as a better fitness score is approached $\mu$ reduces in size and therefore mutations become less common and a final generation is settled upon. In general, optimizations were carried out across 200 generations, with each generation comprising 1024 genomes.

### 2.4.4 Perfect State Transfer via a Coupling Profile in a Linear Chain of Size N=7

The following findings demonstrate the GA's capacity to identify $J_{i,i+1}$ configurations that produce perfect state transfer. We can defend its usage and correctness by comparing the results to established analytical results for PST in a 7-site chain. We start by initializing all the couplings to be uniform as shown in figure 4.
The GA will then optimize $J_{i,i+1}$ until it finds the optimal PST solution, as seen in figure 5 where PST occurs at $t_f = 5.46/J_{max}$. This is in accordance with known results, where a 7-site chain with fixed coupling according to the Christandl profile $J_{i,i+1} = J_0\sqrt{i(N-i)}$ should result in $F(t) = 1$ at $t_f = 5.44/J_{max}$ [37]. We may also tweak the fitness function parameters ($a$, $b$) to obtain quicker times. For example, a focus on a shorter time with a sacrifice in fidelity might be incorporated by modifying the value of $b$, the $N = 7$ optimisation with $b$ set to -1000 gives a transfer time of $4.8/J_{max}$, with a fidelity of 92.6%, this result can be found in the supporting information of ref [33]. Depending on the physical environment, one may choose faster timeframes to totally eliminate decoherence, hence being able to change ($a$, $b$) is vital. Additionally, using this genetic algorithm, perfect state transfer was created at $t_f = 3.8/J_{max}$for a shoelace network, which is 32% quicker than the Christandl coupling profile [33].

In addition to the validated dynamics, the genetic algorithm generates an energy spec-

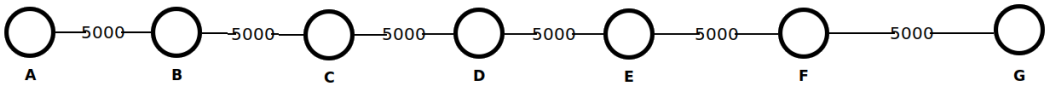


Figure 4: An illustration of the initial spin chain genome. The letters denote the sites, while the numbers between them reflect the neighbour coupling.

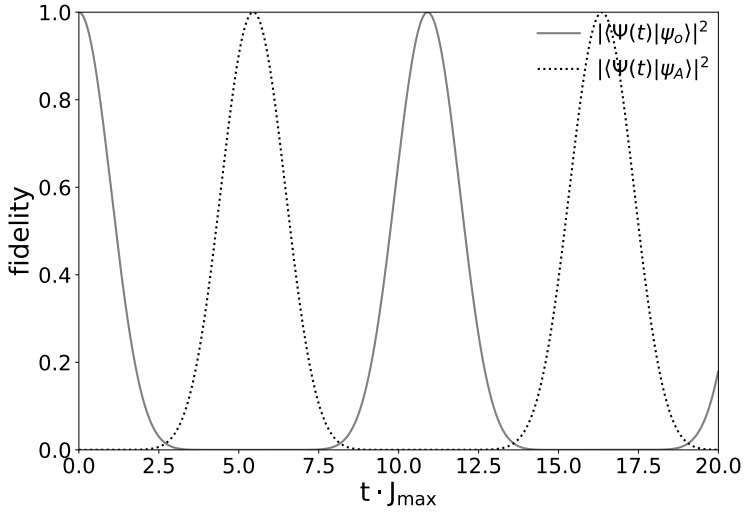


Figure 5: Fidelity vs Time, with $F(t) = 0.9999$. The solid line represents fidelity to the starting state, whereas the dashed line represents fidelity to the desired target state.

trum that is absolutely linear and evenly spaced, as seen in figure 6. This spectrum is also consistent with the findings of Christandl *et al.* [37]. Figure 7 illustrates the generation's lowest, average, and highest fitness scores during the optimization process. The number of mutations decreases visibly with each generation, leading to increasingly precise alterations in fitness. As a result of these findings, we can be certain that the genetic algorithm produces consistent and reliable results, with a demonstrable capacity to discover PST solutions.

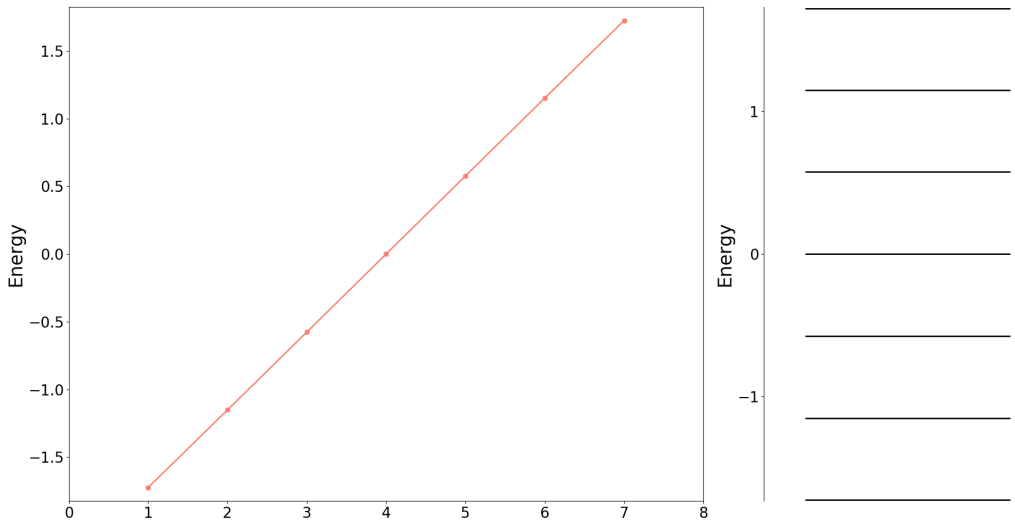


Figure 6: Eigenvalues of $H_{XY}$ with respect to site number, for $F(t) = 0.9999$. The spectrum is linear with equal spacing.

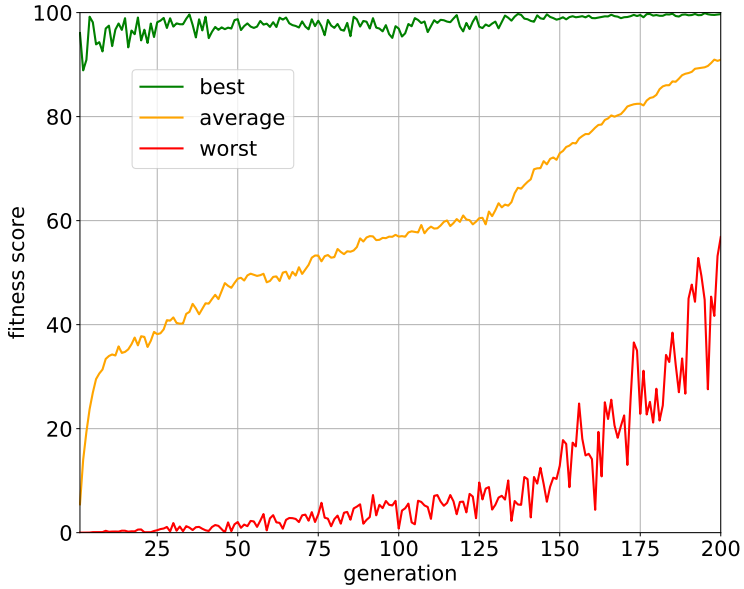


Figure 7: A plot of the worst, average and highest fitness scores for each generation. The size of mutations visibly decreases with each generation, resulting in more precise alterations in fitness.

# 3 Results

In the last decade, theoretical work in spin chains has progressed at great strides in the pursuit to create high-quality information transfer systems for quantum devices. One aspect of spin chains that has been researched extensively is the coupling profiles that achieve perfect state transfer between states. The seminal paper that sparked interest in these systems was by Sougato Bose. Bose discovered that a quantum state in a spin chain with nearest neighbour interaction can be directly transferred with better fidelities than classical transmission throughout the complete length of chains of up to 80 spins in a reasonable amount of time [8]. Herschel Rabitz *et al.* created a technique that finds all possible configurations of couplings that produce PST in XY spin chains. These schemes, without external control fields, only involve pre-engineered couplings, so in many cases, they can be simply realized experimentally [49]. It was also shown that PST can be achieved beyond nearest neighbour coupling. Alastair Kay showed this by including new terms into the spin chain Hamiltonian by solving an inverse eigenvalue problem [50]. Bose *et al.* also investigated unstable spin systems coupled to a bath of spins, which is a step closer to realistic implementations of spin chains [51]. Further work on unstable systems has been done, one of them is the investigation of random fluctuations in coupling [52]. The coupling between sites has been investigated thoroughly; however, the role of on-site energy on perfect state transfer has yet to be substantially investigated. The motive for studying on-site energies is essential since systems with merely tuned couplings might be challenging to obtain. For example, consider the technological difficulties of regulating neighbour interactions with molecules. Leaving the couplings unmodulated while altering the on-site energies may be simpler for some systems, such as ion traps. The capacity to create perfect state transfer solely by modifying the configuration of on-site energy was researched in this study where the connection between sites was kept constant and uniform in all results. PST was identified as a result of the formation of a unique eigenvalue spectrum. In these results, mirror symmetry has been imposed.

## 3.1 PST Optimization of the On-Site Energies in Spin Chains

We begin with a $N = 4$ spin chain where we maintained the couplings constant and unchanged. To discover a perfect state transfer solution, the genetic algorithm was permitted to optimize only the on-site energies. Figure 8(a) depicts the outcome of this optimization on the on-site energies, which has a highly unique structure. The dynamics are also quite unique; note that in figure 8(b) where fidelity as a function of time is plotted, the solid line represents fidelity to the starting state, whereas the dashed line represents fidelity to the desired target state, the dotted line peaks slightly at 2.5 $tJ_{max}$ before $F(t) = 0.9999$. The accompanying energy spectrum is the most fascinating artefact of this consequent optimization, as seen in figure 9, where the spectrum is exactly linear and of equal distance, except for the final two eigenvalues, which are $1/3$ the separation. This is significant since it will be demonstrated that this is a common outcome.

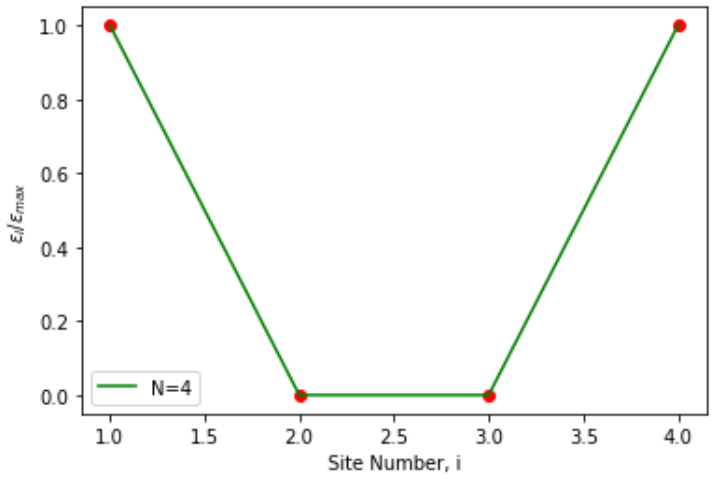


((a)) $\epsilon_i$ vs site number

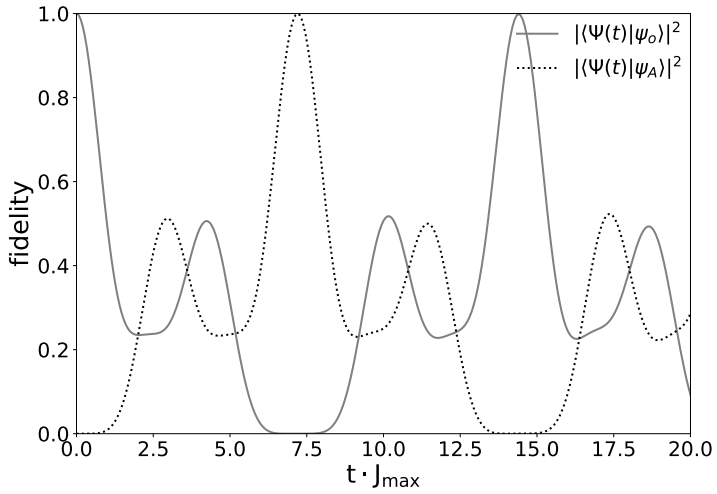


((b)) Dynamics for $N = 4$ showing $F(t) = 99\%$, the solid line represents fidelity to the starting state, whereas the dashed line represents fidelity to the desired target state.

Figure 8: (a) The configuration of fixed $\epsilon_i$ that generates $F(t) = 0.9999$ for $N = 4$, (b) The system dynamics, i.e. the fidelity vs time, demonstrating perfect state transfer for $N = 4$

We next move onto a larger chain beginning with $N = 5$, which produces findings that are consistent with $N = 4$. Only the on-site energies were optimized for perfect state transfer, leaving the coupling between sites unchanged and uniform. Figure 10(a) depicts the configuration of on-site energies chosen by the genetic algorithm for the perfect state transfer solution; curiously, it again chooses a parabolic shape. Figure 10(b) depicts the dynamics of $N = 5$, which displays similar behaviour to that of $N = 4$, with a minor peak before perfect state transfer. Figure 11 also shows that the eigenvalue spectrum is again linear and of equivalent distance, with the exception of the two greatest energies,

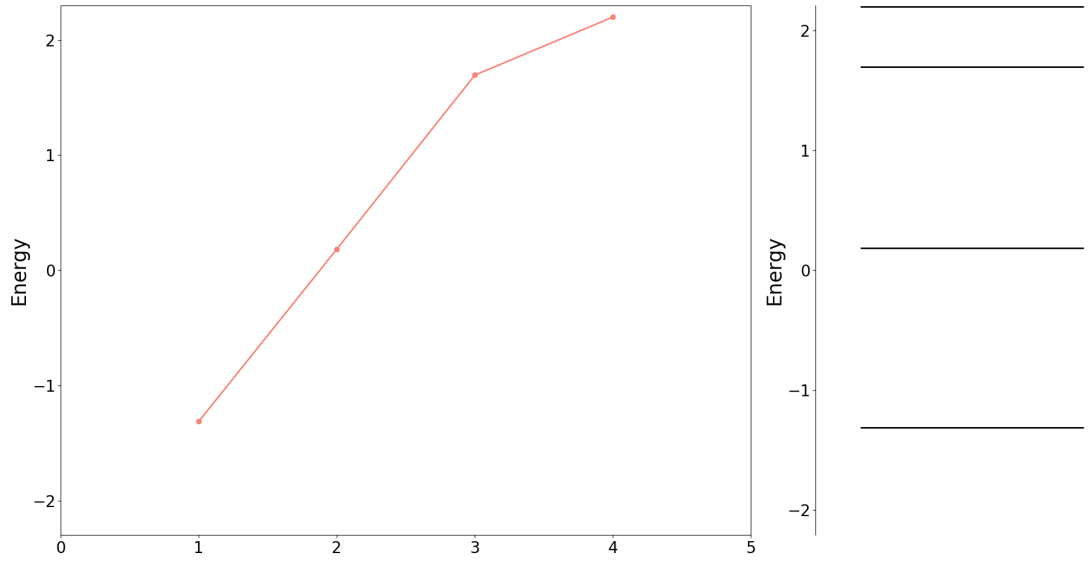


Figure 9: Spectrum of $E_i$ for the N=4 perfect state transfer solution shows that the top highest eigenvalues are not equal in distance to the rest, but are actually 1/3 the distance.

which are 1/3 the separation. Figure 12 demonstrates that $N = 6$ conforms completely with the previous results, and figure 13 shows again the eigenvalue spectrum linear and of equivalent distance, with the exception of the two largest energies, which are 1/3 apart.

As an example of how these results can be explained analytically, consider a spectrum of $E_i$ similar to the perfect state transfer solutions illustrated where all the eigenvalues are of equal separation except for the highest two, which are 1/3 of the separation of the other values

$$E_i = \frac{5}{3}\Delta, \Delta, -\Delta, -3\Delta, \tag{43}$$

with $\Delta$ being some constant. Using equations (29,30) and the spectrum provided, we can thus write the even(+) and odd(-) time-dependent wave functions as

$$|\psi(t)\rangle_+ = a_{5/3\Delta} e^{-i5\Delta t/3} |u_{5/3\Delta}\rangle + a_{-\Delta} e^{i\Delta t} |u_{-\Delta}\rangle , \tag{44}$$

and

$$|\psi(t)\rangle_- = a_{\Delta} e^{-i\Delta t} |u_{\Delta}\rangle + a_{-3\Delta} e^{3i\Delta t} |u_{-3\Delta}\rangle . \tag{45}$$

We can now show such a system can exhibit perfect state transfer. If we substitute $t = 3\pi/2\Delta$ and apply the spectrum (43), the wave function solutions become

$$|\psi(3\pi/2\Delta)\rangle_+ = e^{i3\pi/2}\Big( a_{5/3\Delta} |u_{5/3\Delta}\rangle + a_{-\Delta} |u_{-\Delta}\rangle \Big), \tag{46}$$

and

$$|\psi(3\pi/2\Delta)\rangle_- = -e^{i3\pi/2}\Big( a_{\Delta} |u_{\Delta}\rangle + a_{-3\Delta} |u_{-3\Delta}\rangle \Big). \tag{47}$$

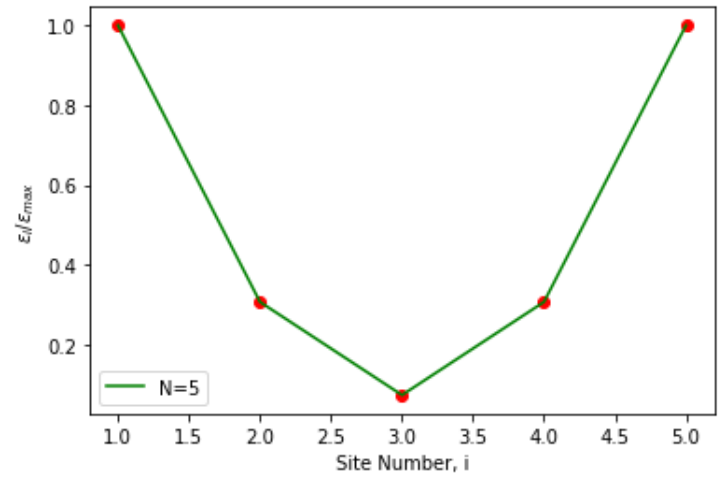


((a)) $\epsilon_i$ vs site number

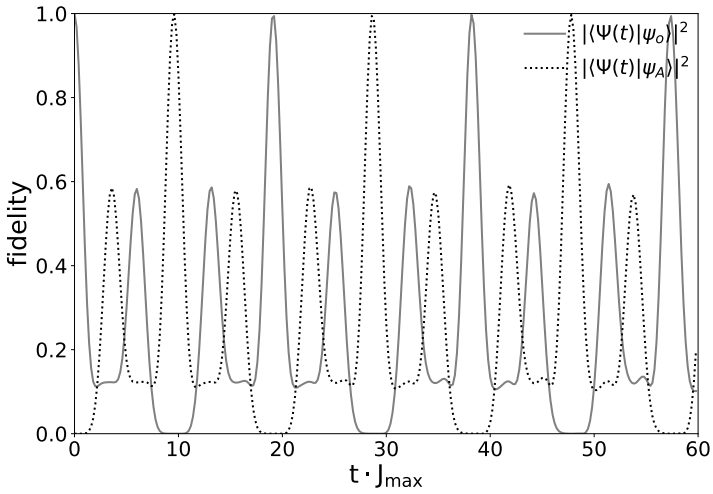


((b)) Dynamics for $N = 5$, $F(t) = 99\%$

Figure 10: (a) A configuration of $\epsilon_i$ that generates $F(t) = 0.9999$ for $N = 5$, (b) The system dynamics, i.e. the fidelity vs time, demonstrating perfect state transfer for $N = 5$. The solid line represents fidelity to the starting state, whereas the dashed line represents fidelity to the desired target state.

The mirroring of equations (46) and (47) occurs because the odd states obtain a negative sign relative to the even states such that the overall state mirrors the centre of the chain. If we refer back to sections 2.2 and 2.3, any state at t=0 has unit fidelity against the mirrored starting state. The mirrored starting state has all the odd components multiplied by -1 relative to the even components, therefore both states will mirror themselves and achieve perfect state transfer. This shows analytically that the spectra discovered by the genetic algorithm for all the $N$ chain solutions may be used to generate systems for perfect state transfer since they produce eigenvalue spectra similar to (43). These spectra appear when the configurations of $\epsilon_i$ are parabolic about the mid-point of the chain. They can

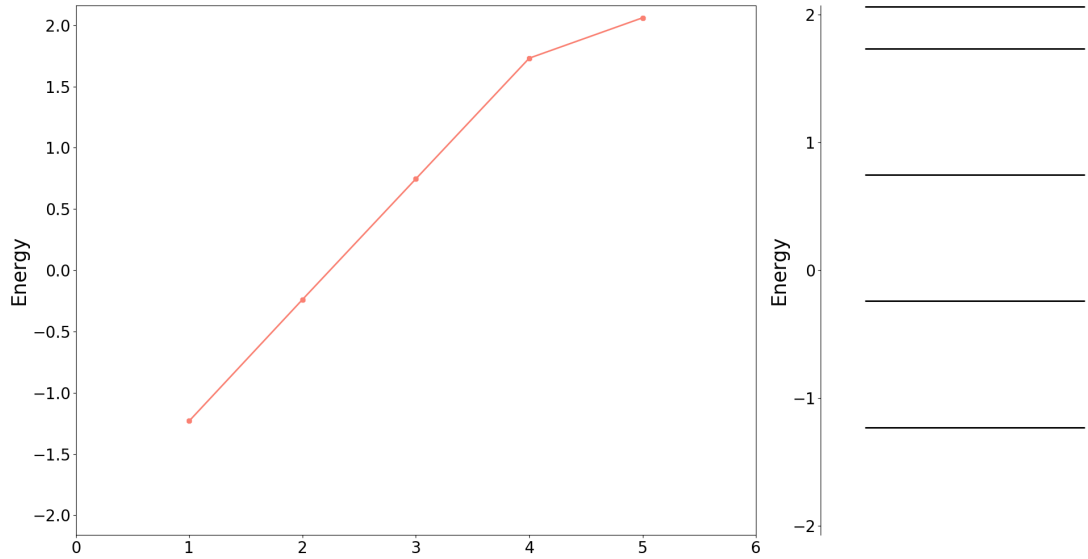


Figure 11: The resulting energy spectrum for the $N = 5$ perfect state transfer solution shows that the top highest eigenvalues are not equal in separation but 1/3 the separation.

be defined such that all eigenvalues are of identical distance except for the top two, where the ratio of this separation is an odd integer, which we denote as $p$,

$$1/p = \frac{d'}{\frac{1}{n}\sum_{i=1}^{n} d_i}, \tag{48}$$

where $d_i = |E_i - E_{i+1}|$ and $d'$ is the difference between the last two eigenvalues.
Table 1 displays the computed 1/p values for each N spin chain solution from the genetic algorithm. It's worth noting that we have $p = 3$ up to N=7. N=7, on the other hand, contains both $p = 3$ and $p = 5$ PST solutions, while N=8 converges towards $p = 5$. One can notice a trend if a larger N is computed, the gap between the top two $E_i$ will diminish, i.e larger $p$. This was not thoroughly examined, but it may be worth more investigation in the future to evaluate the scalability, as it appears that for bigger $p$, times for obtaining perfect state transfer get longer.

| $1/p$ for each N spin chain | |
|---|---|
| Spin chain solutions | $1/p$ |
| $N = 4$ spin chain | 0.33 |
| $N = 5$ spin chain | 0.33 |
| $N = 6$ spin chain | 0.33 |
| $N = 7$ spin chain | 0.29, 0.21 |
| $N = 8$ spin chain | 0.21 |

Table 1: A table includes all the discovered values for 1/p for the various N-size chains, manually computed by equation (48) from the solution's eigenvalue spectrums.

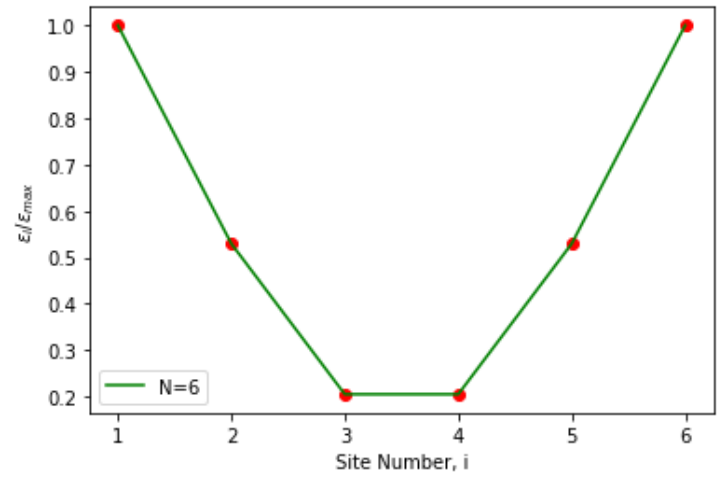


((a)) $\epsilon_i$ vs site number

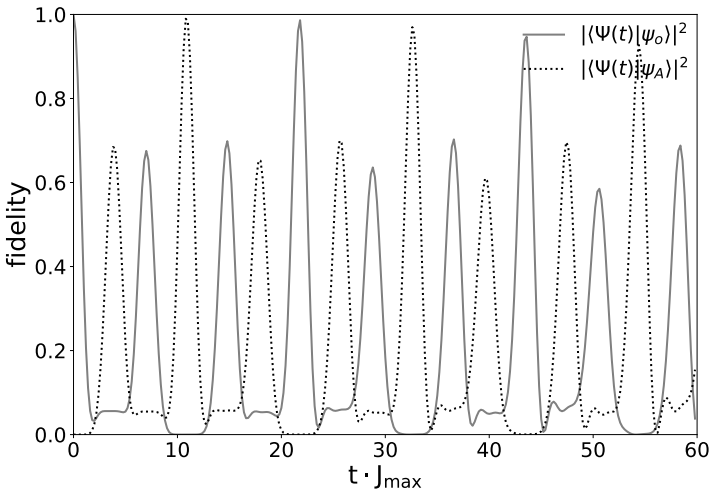


((b)) Dynamics for $N = 6$, $F(t) = 99\%$

Figure 12: (a) The configuration of fixed $\epsilon_i$ that generates $F(t) = 0.9999$ for $N = 6$, (b) The system dynamics, i.e. the fidelity vs time, demonstrating perfect state transfer for $N = 6$. The solid line represents fidelity to the starting state, whereas the dashed line represents fidelity to the desired target state.

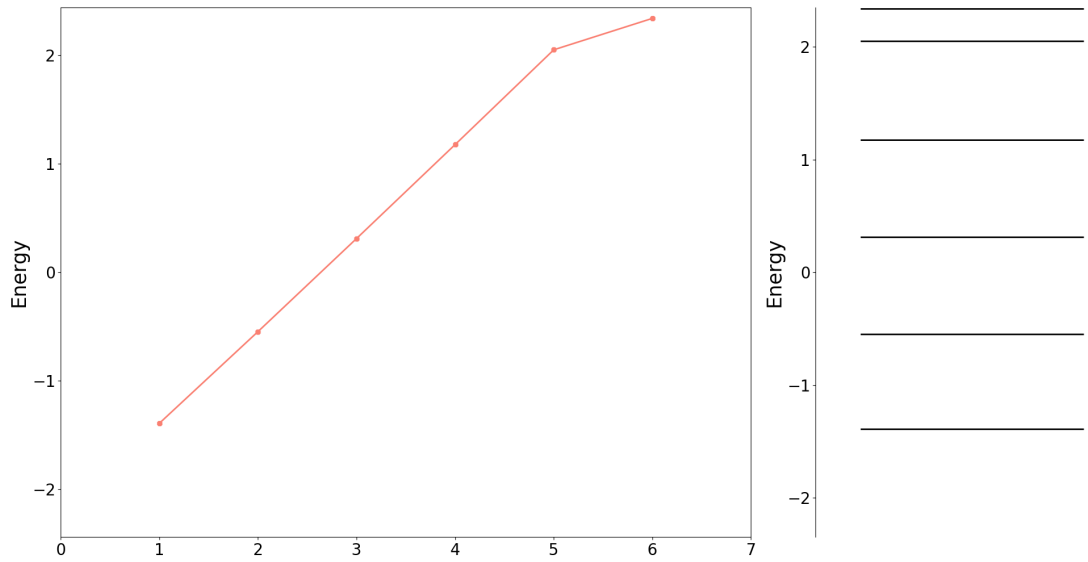


Figure 13: The resulting energy spectrum for the $N = 6$ perfect state transfer solution shows that the top highest eigenvalues are not equal in separation but $1/3$ the separation.

## 3.2 The N=7 Case and Larger N

The example of N=7 is particularly noteworthy since the dynamics vary depending on the timeframe of perfect state transfer. There are two different $p$ solutions for N=7, as shown in table 1 of the preceding section. The solution with two peaks before perfect state transfer 16(b) and another solution with one peak that occurs in a shorter time span 14(b). This may be divided into two respective $p$ solutions for N=7, one for $p = 5$ and one for $p = 3$. It is not confirmed that $N < 7$ cannot have a spectrum that corresponds to $p = 5$. However, we have not come across any such solutions. We may thus utilize the results for N=7 to obtain some insight into bigger N systems. If the genetic algorithm is given free rein to discover a solution without any constraints, such as a time limit, it will inevitably converge to a $p = 5$ solution. However, if the temporal frame is reduced significantly, a solution similar to the dynamics of N=4,5,6 is obtained. The primary distinction between the dynamics of $p = 3$ and $p = 5$ is as follows:

- 1) $p = 5$ takes longer to reach perfect state transfer and has two peaks before reaching maximum fidelity.
- 2) $p = 3$ takes less time to accomplish perfect state transfer and has one peak before reaching maximum fidelity.

Figure 14(a) displays the configuration of on-site energies chosen by the genetic algorithm for the $p = 3$ perfect state transfer solution. Figure 14(b) demonstrates the dynamics of $N = 7$, which exhibits identical features to preceding N chains, with one small peak before perfect state transfer. Figure 15 further indicates that the eigenvalue spectrum is linear and of equivalent distance, except for the two highest energies, which are $1/3$ distance apart. Figure 16(a) depicts the genetic algorithm's selection of on-site energies for the $p = 5$ perfect state transfer solution; notably, it shows a parabolic shape. Figure 16(b) shows the dynamics of $p = 5$, which differs from prior chains in that it has two small peaks before perfect state transfer.

Figure 17 further shows that for $p = 5$, with the exception of the two highest energies, the eigenvalue spectrum is linear and of equivalent distance. The dynamics presented may be explained by referring to the preceding analytical explanation in 3.1. In terms of the spectrum spacing, equations 46 and 47 show how long it takes for all the odd eigenstates to acquire (-1) compared to all the even eigenstates.

This would explain why $p = 3$ solutions make one effort before perfect state transfer since it will make an attempt at $\pi/2\Delta$, but $p = 5$ solutions make two attempts. As a result, we may expect that for greater $p$, i.e. smaller energy gaps at the top, several attempts would be required before perfect state transfer would be achieved, requiring more time. Figure 18(a) and 18(b) reveal the $N = 8$ results which naturally converge to $p = 5$ and exhibit the same properties as the $p = 5$ solution of $N = 7$. Furthermore, the timing at which perfect state transfer transpires is particularly interesting. When we split these various

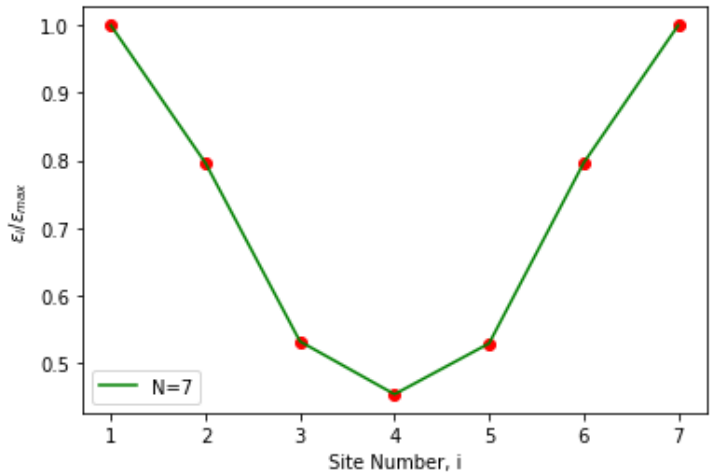


((a)) $\epsilon_i$ vs site number.

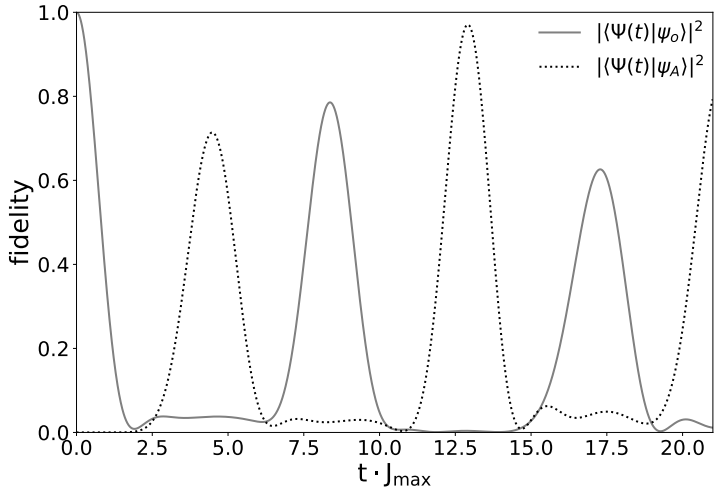


((b)) Dynamics for $N = 7$, $F(t) = 98\%$

Figure 14: (a) The configuration of fixed $\epsilon_i$ for $N = 7$, (b) The system dynamics, i.e. the fidelity vs time, demonstrating perfect state transfer for $N = 7$ with $p = 3$. The solid line represents fidelity to the starting state, whereas the dashed line represents fidelity to the desired target state.

$p$ solution types into families, we can observe a pattern develop in the time it takes for perfect state transfer to occur. Figure 20 depicts this trend, where the time required to achieve perfect state transfer rises linearly with the number of sites in the chain. Notably, the $p = 5$ solutions for $N = 7$ and $N = 8$ increase linearly with a different slope to the $p = 3$ solutions. It could be interesting to look into these $p$ "families" further by taking into account greater $N$. Unfortunately, this was not investigated further in this study.

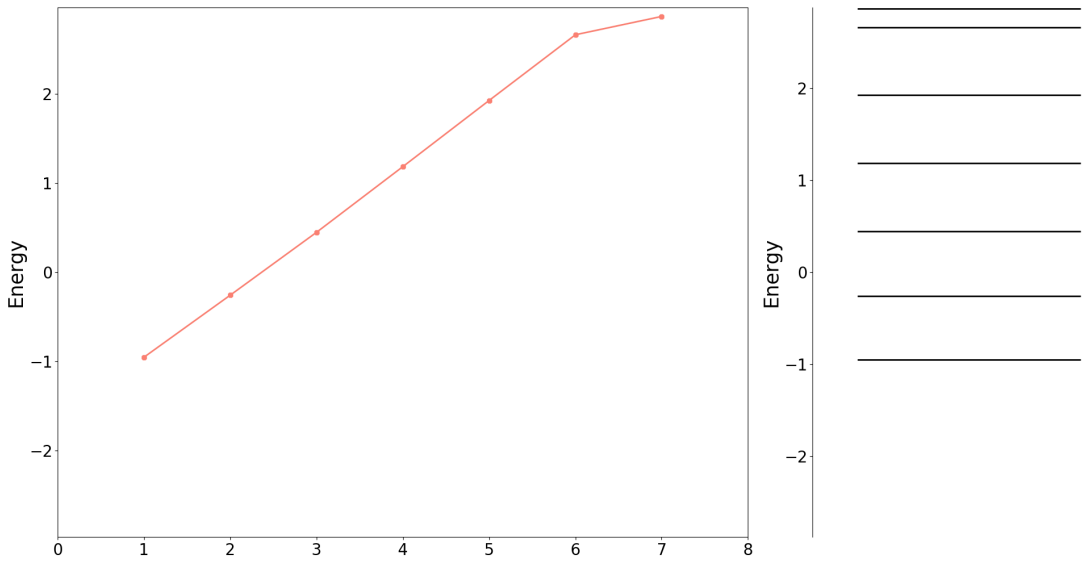


Figure 15: The resulting energy spectrum for the $N = 7$ solution with $p = 3$.

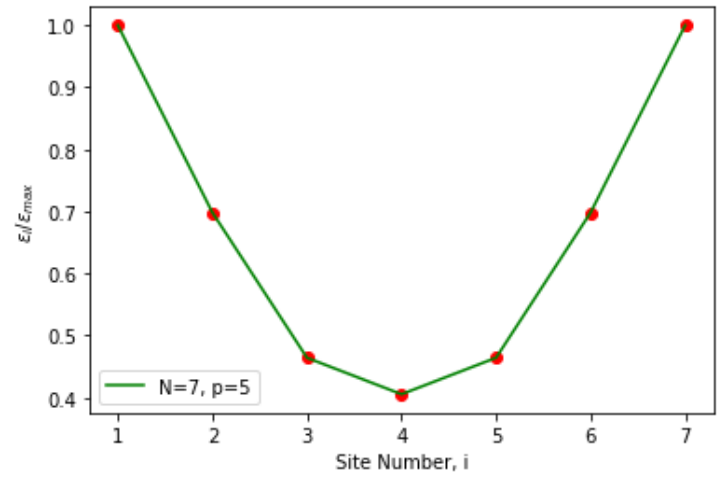


((a)) $\epsilon_i$ vs site number.

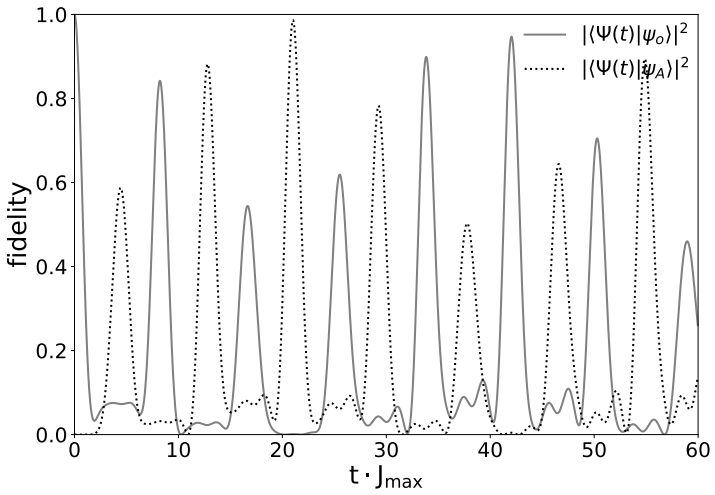


((b)) Dynamics for $N = 7$ and $p = 5$ with $F(t) = 98\%$

Figure 16: (a) The configuration of fixed $\epsilon_i$ for $N = 7$, (b) The system dynamics, i.e. the fidelity vs time, demonstrating perfect state transfer for $N = 7$. The solid line represents fidelity to the starting state, whereas the dashed line represents fidelity to the desired target state.

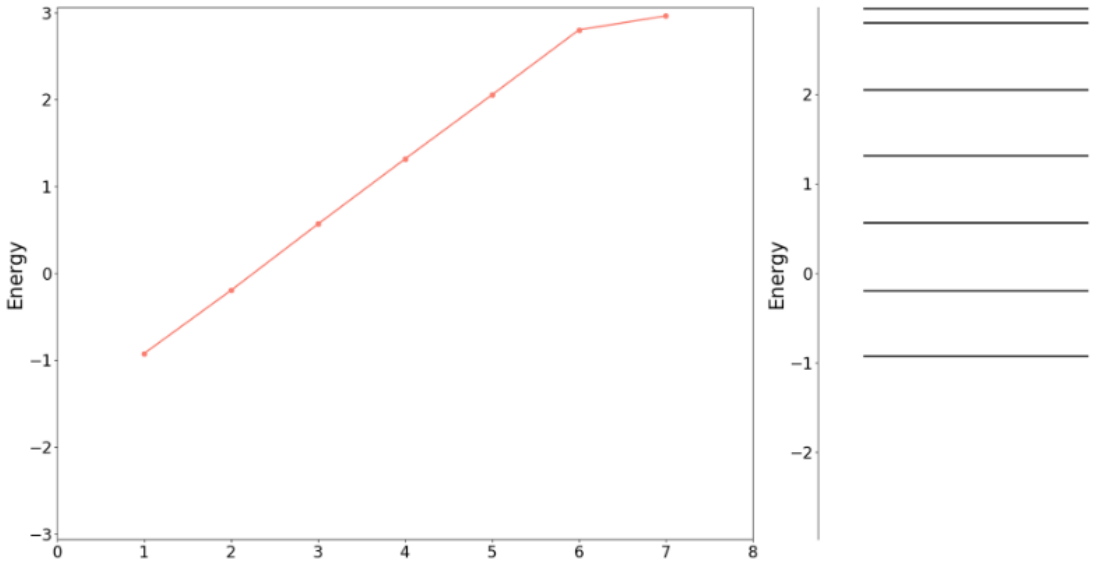


Figure 17: The resulting energy spectrum for the $N = 7$ solution with $p = 5$.

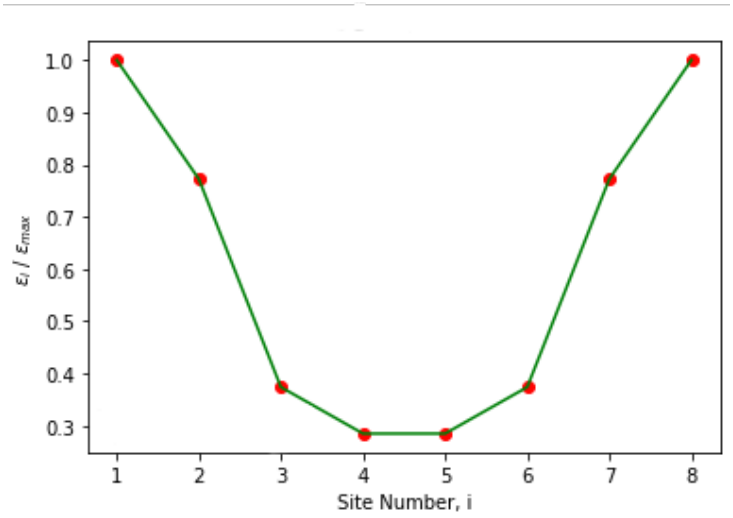


((a)) $\epsilon_i$ vs site number.

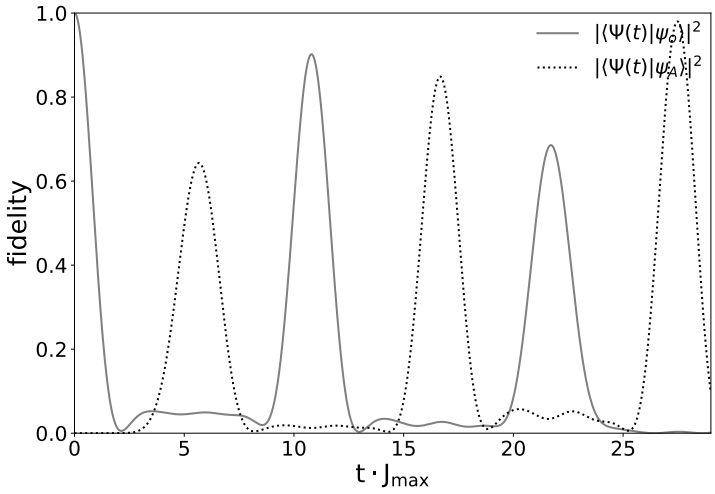


((b)) Dynamics for $N = 8$, $p = 5$

Figure 18: (a) The configuration of fixed $\epsilon_i$ for $N = 8$, (b) The system dynamics, i.e. the fidelity vs time, demonstrating perfect state transfer for $N = 8$. The solid line represents fidelity to the starting state, whereas the dashed line represents fidelity to the desired target state.

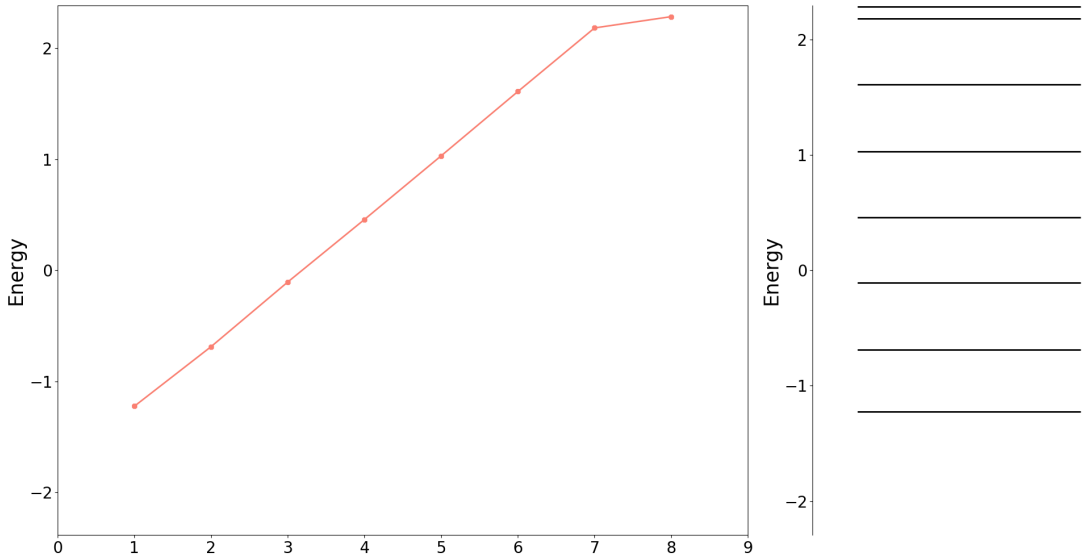


Figure 19: The resulting energy spectrum for the $N = 8$ showing a $p = 5$.

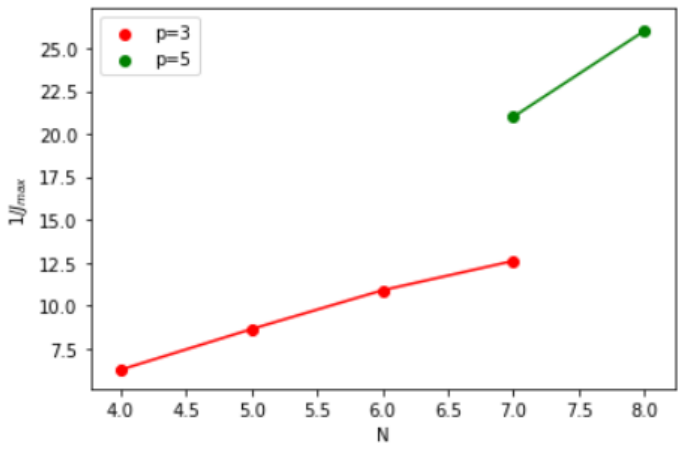


Figure 20: A graph of the perfect state transfer time for each N chain solution, demonstrating an approximate linear rise with each N and a separate branch for $p = 5$ solutions.

# 4 Conclusions

In this work, we demonstrated that, given the correct spectrum, perfect state transfer is achievable by adjusting only the diagonal elements of the XY Hamiltonian. This is important because systems with only tuned couplings may be difficult to achieve for some physical implementations. The genetic algorithm was also highly valuable in this research, demonstrating that combining A.I and physics may provide promising results and, in the future, may aid us in investigating far larger research problems. Figure 21 shows all the configurations found for $\epsilon_i$ that generate PST which follows a clear reoccurring pattern. We also introduced a class of eigenvalue spectra which we denoted as $p$ types, in which $1/p$ is the ratio of separation to the other eigenvalues and perfect state transfer is feasible if $p$ is an odd integer. Additionally, we found that larger $p$ systems will make more attempts before reaching PST and thus require more time to reach PST. Furthermore, in the case of $N = 7$, a perturbation theory argument may explain how the $p = 3$ and $p = 5$ solutions for N=7 are related since 14(a) and 16(a) differ mainly by the first and last on-site energies. Furthermore, additional research into the scalability of these systems might be conducted by considering that for larger N systems, the gap between the top two $E_i$ would narrow. It appears that for larger $p$, timeframes for attaining perfect state transfer become longer. Despite the consideration of ideal systems in this study and the

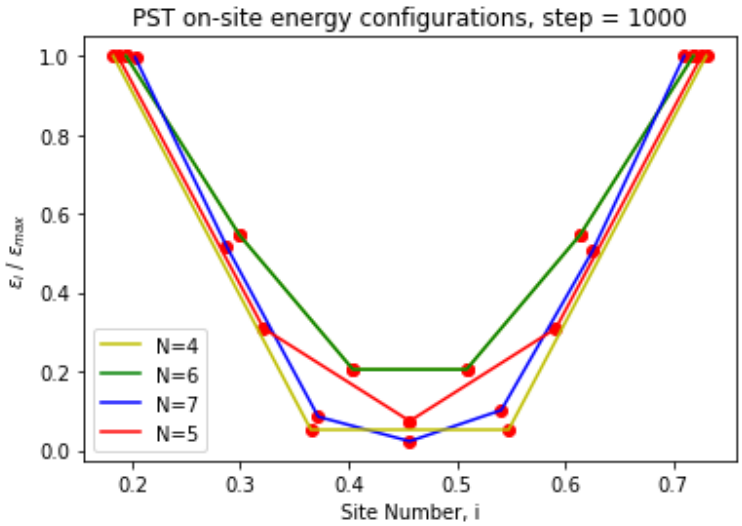


Figure 21: All on-site energy configurations for all the N PST solutions.

inherent robustness of spin-chain natural dynamics against information loss, it is important to acknowledge that the performance of spin-chain protocols can still be affected by quantum noise and fluctuations. There are remediation strategies, such as Alastair Kay's proposed Calderbank-Shor-Steane code [53], dynamical decoupling, that employs strong static and oscillating control fields to suppress interaction between the spin chain and the environment [54], and topologically protected states, which exhibit remarkable resilience against random noise [55]. These studies shed light on spin chains' robustness, demon-

strating their capacity to endure and reduce the disruptive effects of noise. It should be noted that the specific impact of noise and fluctuations is contingent upon the particular spin chain protocol employed, as different protocols leverage diverse types of spins (e.g., electron spins, nuclear spins), interactions (e.g., nearest-neighbour, long-range), and operations (e.g., single-qubit gates, multi-qubit gates). These factors significantly influence protocol sensitivity to noise and fluctuations, requiring careful consideration in spin chain system design and analysis.

Finally, the hope is that the research presented in this thesis will bring us one small step closer to understanding the various ways spin chains may be employed as quantum wires. We can physically realize these systems and tune the on-site energies by adjusting external fields, which is sometimes easier than adjusting coupling strength, thus adding another tool to our toolkit for implementing PST spin chain systems. In any case, there is a lot more to learn, not just about the topics presented in this thesis, but about quantum information processing systems in general.

# 5 Appendix

# 6 GA Parameters used for $N = 4, 5, 6, 7$

## 6.1 $N = 4, 5, 6, 7$ and $p = 3$

- cores = 1
- generations = 200
- genomes per generation = 1024
- mutate chance = 1.000
- intial mutate amount = 2000
- final mutate amount = 1
- use linear scaling = F
- only change energies = T

## 6.2 $N = 7, 8$, and $p = 5$

- cores = 1
- generations = 400
- genomes per generation = 2048
- mutate chance = 1.000
- intial mutate amount = 2000
- final mutate amount = 1
- use linear scaling = F
- only change energies = T

# References


[1] Richard P Feynman. Simulating physics with computers. *International journal of theoretical physics*, 21(6/7):467–488, 1982.

[2] David Deutsch and Richard Jozsa. Rapid Solution of Problems by Quantum Computation. *Proceedings of the Royal Society of London Series A*, 439(1907):553–558, December 1992.

[3] Daniel R. Simon. On the power of quantum computation. *SIAM Journal on Computing*, 26(5):1474–1483, 1997.

[4] Peter W. Shor. Polynomial-time algorithms for prime factorization and discrete logarithms on a quantum computer. *SIAM Journal on Computing*, 26(5):1484–1509, oct 1997.

[5] Charles H. Bennett, Gilles Brassard, Claude Crépeau, Richard Jozsa, Asher Peres, and William K. Wootters. Teleporting an unknown quantum state via dual classical and einstein-podolsky-rosen channels. *Phys. Rev. Lett.*, 70:1895–1899, Mar 1993.

[6] Charles H. Bennett and Gilles Brassard. Quantum cryptography: Public key distribution and coin tossing. *Theoretical Computer Science*, 560:7–11, dec 2014.

[7] Yang Fan. Conditional quantum cnot gate between two four-level atoms. *Chin. Opt. Lett.*, 3(3):176–178, Mar 2005.

[8] Sougato Bose. Quantum communication through an unmodulated spin chain. *Physical Review Letters*, 91(20), nov 2003.

[9] Tobias J. Osborne and Noah Linden. Propagation of quantum information through a spin system. *Phys. Rev. A*, 69:052315, May 2004.

[10] R. Ronke, I. D'Amico, and T. P. Spiller. Knitting distributed cluster-state ladders with spin chains. *Physical Review A*, 84(3), sep 2011.

[11] J. Eisert, M. B. Plenio, S. Bose, and J. Hartley. Towards quantum entanglement in nanoelectromechanical devices. *Phys. Rev. Lett.*, 93:190402, Nov 2004.

[12] Vittorio Giovannetti and Rosario Fazio. Information-capacity description of spin-chain correlations. *Phys. Rev. A*, 71:032314, Mar 2005.

[13] Irene D'Amico, Brendon W. Lovett, and Timothy P. Spiller. Creating and preserving multi-partite entanglement with spin chains. *physica status solidi c*, 5(7):2481–2485, may 2008.

[14] Daniel Burgarth and Sougato Bose. Conclusive and arbitrarily perfect quantum-state transfer using parallel spin-chain channels. *Phys. Rev. A*, 71:052315, May 2005.

[15] Ying Li, Tao Shi, Bing Chen, Zhi Song, and Chang-Pu Sun. Quantum-state transmission via a spin ladder as a robust data bus. *Phys. Rev. A*, 71:022301, Feb 2005.

[16] Tao Shi, Ying Li, Zhi Song, and Chang-Pu Sun. Quantum-state transfer via the ferromagnetic chain in a spatially modulated field. *Phys. Rev. A*, 71:032309, Mar 2005.

[17] Martin B Plenio and Fernando L Semiã o. High efficiency transfer of quantum information and multiparticle entanglement generation in translation-invariant quantum chains. *New Journal of Physics*, 7:73–73, mar 2005.

[18] Rebecca Ronke, Tim Spilled, and Irene D'Amico. Long-range interactions and information transfer in spin chains. *Journal of Physics: Conference Series*, 286:012020, mar 2011.

[19] C. R. Monroe D. Kielpinski and D.J. Wineland. Architecture for a large-scale ion-trap quantum computer. *Nature*, 417, 2002.

[20] A Lyakhov and C Bruder. Quantum state transfer in arrays of flux qubits. *New Journal of Physics*, 7:181–181, aug 2005.

[21] A. O. Lyakhov and C. Bruder. Use of dynamical coupling for improved quantum state transfer. *Phys. Rev. B*, 74:235303, Dec 2006.

[22] Alessandro Romito, Rosario Fazio, and C. Bruder. Solid-state quantum communication with josephson arrays. *Phys. Rev. B*, 71:100501, Mar 2005.

[23] Navin Khaneja and Steffen J. Glaser. Efficient transfer of coherence through ising spin chains. *Phys. Rev. A*, 66:060301, Dec 2002.

[24] John L. Gustafson. *Moore's Law*, pages 1177–1184. Springer US, Boston, MA, 2011.

[25] Michael A. Nielsen and Isaac L. Chuang. *Quantum Computation and Quantum Information: 10th Anniversary Edition*. Cambridge University Press, 2010.

[26] Valerio Scarani, Helle Bechmann-Pasquinucci, Nicolas J. Cerf, Miloslav Dušek, Norbert Lütkenhaus, and Momtchil Peev. The security of practical quantum key distribution. *Rev. Mod. Phys.*, 81:1301–1350, Sep 2009.

[27] Marco Fellous-Asiani, Jing Hao Chai, Robert S. Whitney, Alexia Auffèves, and Hui Khoon Ng. Limitations in quantum computing from resource constraints. *PRX Quantum*, 2:040335, Nov 2021.

[28] I. L. Chuang, R. Laflamme, P. W. Shor, and W. H. Zurek. Quantum computers, factoring, and decoherence. *Science*, 270(5242):1633–1635, 1995.

[29] Abdullah Ash Saki, Mahabubul Alam, and Swaroop Ghosh. Study of decoherence in quantum computers: A circuit-design perspective, 2019.

[30] C. Macchiavello, S. F. Huelga, J. I. Cirac, A. K. Ekert, and M. B. Plenio. *Decoherence and Quantum Error Correction in Frequency Standards*, pages 337–345. Springer US, Boston, MA, 2002.

[31] David P. DiVincenzo. The physical implementation of quantum computation. *Fortschritte der Physik*, 48(9-11):771–783, sep 2000.

[32] J Elzerman, R Hanson, Laurens Willems van Beveren, B Witkamp, L Vandersypen, and L Kouwenhoven. Single-shot read-out of an individual electron spin in a quantum dot. nature 430. *Nature*, 430:431–5, 08 2004.

[33] Luke Mortimer, Marta P. Estarellas, Timothy P. Spiller, and Irene D'Amico. Evolutionary computation for adaptive quantum device design. *Advanced Quantum Technologies*, 4(8):2100013, 2021.

[34] Jonathan Allcock and Noah Linden. Quantum communication beyond the localization length in disordered spin chains. *Phys. Rev. Lett.*, 102:110501, Mar 2009.

[35] Joachim Stolze, Gonzalo A. Álvarez, Omar Osenda, and Analia Zwick. *Robustness of Spin-Chain State-Transfer Schemes*, pages 149–182. Springer Berlin Heidelberg, Berlin, Heidelberg, 2014.

[36] Matthias Christandl, Nilanjana Datta, Artur Ekert, and Andrew J. Landahl. Perfect state transfer in quantum spin networks. *Phys. Rev. Lett.*, 92:187902, May 2004.

[37] Matthias Christandl, Nilanjana Datta, Tony C. Dorlas, Artur Ekert, Alastair Kay, and Andrew J. Landahl. Perfect transfer of arbitrary states in quantum spin networks. *Phys. Rev. A*, 71:032312, Mar 2005.

[38] T. Baeck, D.B. Fogel, and Z. Michalewicz. *Evolutionary Computation 1: Basic Algorithms and Operators*. Basic algorithms and operators. Taylor & Francis, 2000.

[39] John H. Holland. Genetic algorithms. *Scientific American*, July 1992.

[40] J.R. Koza, D. Andre, M.A. Keane, and F.H. Bennett. *Genetic Programming III: Darwinian Invention and Problem Solving*. Bradford book. Morgan Kaufmann, 1999.

[41] Z. Michalewicz. *Genetic algorithms + data structures = evolution programs (3nd, extended ed.)*. Springer-Verlag New York, Inc., New York, NY, USA, 1996.

[42] Melanie Mitchell. *An Introduction to Genetic Algorithms*. MIT Press, Cambridge, MA, USA, 1998.

[43] M. Mitchell. *An Introduction to Genetic Algorithms*. Complex Adaptive Systems. MIT Press, 1998.

[44] C.R. Stephens, M. Toussaint, P.F. Stadler, and D. Whitley. *Foundations of Genetic Algorithms: 9th International Workshop, FOGA 2007, Mexico City, Mexico, January 8-11, 2007, Revised Selected Papers*. ACM Digital Library. Springer, 2007.

[45] N. Horta, M.B. Barros, J. Silva, and G. Neves. Enhanced genetic algorithm kernel applied to a circuit-level optimization e-design environment. In *IEEE Conf. on Electronics, Circuits and System*, pages –, December 2003.

[46] Mitsuru Honda. Application of genetic algorithms to modelings of fusion plasma physics. *Computer Physics Communications*, 231:94–106, 2018.

[47] Jonathan Wright and Ali Alajmi. The robustness of genetic algorithms in solving unconstrained building optimisation problems. *Proceedings of the 7th IBPSA Conference: Building Simulation*, 01 2005.

[48] U. Las Heras, U. Alvarez-Rodriguez, E. Solano, and M. Sanz. Genetic algorithms for digital quantum simulations. *Phys. Rev. Lett.*, 116:230504, Jun 2016.

[49] Yaoxiong Wang, Feng Shuang, and Herschel Rabitz. All possible coupling schemes in xy spin chains for perfect state transfer. *Physical Review. A*, 84, 01 2011.

[50] Alastair Kay. Perfect state transfer: Beyond nearest-neighbor couplings. *Phys. Rev. A*, 73:032306, Mar 2006.

[51] Daniel Burgarth and Sougato Bose. Universal destabilization and slowing of spin-transfer functions by a bath of spins. *Phys. Rev. A*, 73:062321, Jun 2006.

[52] D. Kong and An Min Wang. Quantum-state transfer on spin-chain channels with random imperfection. *The European Physical Journal D*, 55:211–221, 10 2009.

[53] Alastair Kay. Quantum error correction for state transfer in noisy spin chains. *Physical Review A*, 93(4), apr 2016.

[54] Sharoon Austin, Muhammad Qasim Khan, Maryam Mudassar, and Adam Zaman Chaudhry. Continuous dynamical decoupling of spin chains: Modulating the spin-environment and spin-spin interactions. *Phys. Rev. A*, 100:022102, Aug 2019.

[55] Marta P. Estarellas, Irene D'Amico, and Timothy P. Spiller. Topologically protected localised states in spin chains. *Scientific Reports*, 7(1), feb 2017.